Voprosy Onkologii = Problems in Oncology. 2025. Vol. 71, No 4
UDC 616.5-006.81
DOI 10.37469/0507-3758-2025-4-OF-2448

© *Aleksei V. Novik[1,2], Kristina Yu. Kapusta[1], Tatiana L. Nekhaeva[1], Anna B. Danilova[1], Andrey V. Orekhov[3], Egor V. Vasiliev[3], Dilorom Kh. Latipova[1,2], Anna I. Semenova[1], Lilia S. Baboshkina[1], Gulfiya M. Teletaeva[1], Tatiana Yu. Semiglazova[1,4], Irina A. Baldueva[1]*

Joint Analysis of the Interferon Gene Signatures and Cancer-Testis Gene Expression in Cutaneous Melanoma Patients*

[1]N.N. Petrov National Medicine Research Center of Oncology, St. Petersburg, the Russian Federation
[2]St. Petersburg State Pediatric Medical University, St. Petersburg, the Russian Federation
[3]Saint Petersburg State University, St. Petersburg, the Russian Federation
[4]North-Western State Medical University named after I.I. Mechnikov, St. Petersburg, the Russian Federation

© *А.В. Новик[1,2], К.Ю. Капуста[1], Т.Л. Нехаева[1], А.Б. Данилова[1], А.В. Орехов[3], Е.В. Васильев[3], Д.Х. Латипова[1,2], А.И. Семенова[1], Л.С. Бабошкина[1], Г.М. Телетаева[1], Т.Ю. Семиглазова[1,4], И.А. Балдуева[1]*

Анализ соответствий сигнатуры генов интерферона и экспрессии раково-тестикулярных генов у больных меланомой кожи**

[1]Федеральное государственное бюджетное учреждение «Национальный медицинский исследовательский центр онкологии имени Н.Н. Петрова» Министерства здравоохранения Российской Федерации, Санкт-Петербург, Российская Федерация
[2]Федеральное государственное бюджетное образовательное учреждение высшего образования «Санкт-Петербургский государственный педиатрический медицинский университет» Министерства здравоохранения Российской Федерации, Санкт-Петербург, Российская Федерация
[3]Федеральное государственное бюджетное образовательное учреждение высшего образования «Санкт-Петербургский государственный университет, Санкт-Петербург, Российская Федерация
[4]Федеральное государственное бюджетное образовательное учреждение высшего образования «Северо-Западный государственный медицинский университет имени И.И. Мечникова» Министерства здравоохранения Российской Федерации, Санкт-Петербург, Российская Федерация

Introduction. Cutaneous melanoma currently lacks well-established molecular biomarkers for predicting immunotherapy response. Emerging candidates under investigation include interferon-stimulated gene (ISG) signatures and cancer-testis antigen (CTA) expression profiles.

Aim. The study performed to characterize the interplay between ISG signatures and CTA expression patterns in cutaneous melanoma patients.

Materials and Methods. The study utilized normalized whole-genome sequencing data comprising expression levels of 43,000 genes from 457 cutaneous melanoma patients, sourced from the publicly available University of California Santa Cruz (UCSC) dataset. Our analysis focused on rhabdoid-testicular CTA genes (n = 186) and interferon-dependent ISG genes (n = 66), the latter analyzed as both full and brief signatures. We performed agglomerative hierarchical clustering via Ward's method separately for ISG and CTA groups. Statistical evaluation of cluster interactions employed seven complementary measures: Pearson's chi-square test, lambda coefficient, contingency coefficient, phi coefficient, Goodman and Kruskal's tau, uncertainty coefficient, and column proportion analysis.

Results. Analysis revealed four conserved ISG clusters across both datasets (two demonstrating high gene expression and two with low expression) showing strong correlation ($\lambda = 0.666$, $p < 0.0001$). For CTA genes, hierarchical clustering identified six primary clusters (two each of high, medium,

Введение. В настоящее время не существует однозначно установленного молекулярного биомаркера для прогнозирования ответа на иммунотерапию у пациентов с меланомой кожи. Изучаются несколько потенциальных биомаркеров, включая сигнатуры генов интерферона (ISG) и экспрессию раково-тестикулярных антигенов (CTA).

Цель. Исследование для оценки взаимодействия между ISG и паттернами CTA у пациентов с меланомой кожи.

Материалы и методы. В работе использованы нормализованные данные полногеномного секвенирования, включающие уровни экспрессии 43 000 генов у 457 пациентов с кожной меланомой из открытых источников набора данных Калифорнийского университета в Санта-Крузе (UCSC).

Для анализа были выбраны раково-тестикулярные антигены CTA (n = 186) и интерферон-стимулированные гены ISG (n = 66); последние представлены как в полной, так и в сокращенной версии. Агломеративная кластеризация генов с использованием метода Уорда была выполнена отдельно для каждого набора генов. Статистический анализ взаимосвязей между кластерами включал следующие методы: критерий χ^2 Пирсона, коэффициент лямбда, коэффициент контингенции, коэффициент фи, τ Гудмана — Краскела, коэффициент неопределенности и анализ пропорций в столбцах.

Результаты. В полном и кратком наборах ISG обнаружено четыре кластера (два кластера генов с высокой и два кластера с низкой экспрессией), которые были сильно коррелированы (λ 0,666, $p < 0,0001$). На первом уровне кластеризации найдено шесть кластеров CTA (два с вы-

* The article contains an online application that contains additional materials https://voprosyonkologii.ru/index.php/journal/article/view/4-25-Joint-Analysis
** Статья содержит онлайн-приложение, в котором размещены дополнительные материалы https://voprosyonkologii.ru/index.php/journal/article/view/4-25-Joint-Analysis

DOI 10.37469/0507-3758-2025-4-OF-2448

and low expression genes) at the first level, which further differentiated into ten subclusters at the third clustering level. Initial comparison of first-level ISG and CTA clusters showed no significant association ($p > 0.1$). Evaluation of third-level CTA clusters against the brief ISG signature demonstrated a weak relationship (symmetric uncertainty coefficient = 0.031, $p = 0.003$). Only two third-level CTA clusters exhibited meaningful associations with ISG patterns: one characterized by minimal CTA expression coupled with high ISG activity, and another showing the inverse relationship of elevated CTA expression paired with low ISG signature.

Conclusion. This study confirms our prior findings regarding the heterogeneous expression profile of CTA in cutaneous melanoma. The majority of CTA clusters demonstrated no significant association with ISG signatures. The identification of specific CTA-ISG expression patterns as predictive biomarkers for immunotherapy response in melanoma patients warrants deeper investigation.

Keywords: interferon gene signatures; cancer-testis antigens; melanoma; cluster analysis

For Citation: Aleksei V. Novik, Kristina Yu. Kapusta, Tatiana L. Nekhaeva, Anna B. Danilova, Andrey V. Orekhov, Egor V. Vasiliev, Dilorom Kh. Latipova, Anna I. Semenova, Lilia S. Baboshkina, Gulfiya M. Teletaeva, Tatiana Yu. Semiglazova, Irina A. Baldueva. Joint analysis of the interferon gene signatures and cancer-testis gene expression in cutaneous melanoma patients. *Voprosy oncologii = Problems in Oncology.* 2025; 71(4): 789-798.-DOI: 10.37469/0507-3758-2025-4-OF-2448

сокой, два со средней и два с низкой экспрессией генов), на третьем уровне — десять кластеров. Кластеры ISG и CTA не были связаны при сравнении на первом уровне кластеризации ($p > 0,1$). Сравнение третьего уровня кластеров CTA с краткой ISG показало слабую ассоциацию между двумя параметрами (симметричный коэффициент неопределенности 0,031, $p = 0,003$). Только два кластера CTA третьего уровня показали связь с ISG: один — с минимальной экспрессией CTA и высокой ISG, второй — с высокой экспрессией CTA и низкой ISG.

Выводы. Результаты исследования подтвердили наши предыдущие находки относительно профиля экспрессии CTA. Большинство кластеров не имели отношения к ISG. Необходимы дальнейшие исследования для понимания возможной роли паттернов экспрессии CTA и ISG в качестве прогностических и предиктивных факторов для иммунотерапии.

Ключевые слова: сигнатура гена интерферона; раково-тестикулярные антигены; меланома; кластерный анализ

✉ Correspondence: Kristina Yu. Kapusta, deulina-97@mail.ru

Introduction

The identification of reliable molecular biomarkers for predicting immunotherapy response in melanoma patients, particularly in the neoadjuvant setting, remains an unmet clinical need. Among currently investigated candidates, interferon gene signatures (ISG) show particular promise. For instance, the OpACIN-neo study identified a 10-gene IFN-γ signature as a prognostic baseline biomarker of pathological response in stage III melanoma patients receiving neoadjuvant combination immunotherapy [1]. Multiple studies have since developed various interferon signatures, suggesting their potential as established biomarkers [2–4]. Notably, patients exhibiting low IFN-γ levels demonstrate reduced likelihood of achieving pathological response and increased risk of disease recurrence compared to those with high IFN-γ expression.

Cancer-testis antigens (CTA) represent another promising class of immunotherapy response biomarkers [5]. These antigens, normally expressed primarily in germ cells in healthy individuals, can also be expressed by tumor cells. Their tumor-specific expression pattern and immunogenic properties make them attractive targets for immunotherapy [6], with over 270 CTAs currently identified [6, 7].

Our previous research demonstrated consistent CTA expression patterns across various tumor types and identified distinct expression clusters [7]. While these findings require validation, no data currently exist regarding potential interactions between CTA clusters and established immunological markers, particularly interferon-dependent gene expression. To address this knowledge gap and confirm our initial observations, we performed a comprehensive analysis of an external gene expression dataset to investigate possible correlations between CTA expression patterns and interferon gene signatures.

Materials and Methods

This study utilized publicly available genomic data from the University of California Santa Cruz (UCSC) Xena database [8], comprising normalized expression levels of 43,000 genes obtained through whole-genome sequencing of 457 cutaneous melanoma tumor samples. Our analysis focused on CTA ($n = 186$) and interferon-stimulated genes (ISG) ($n = 66$), as detailed in Table 1.

The CTA gene panel was compiled through comprehensive searches of CTAbase [9, 10], including the following established antigens: *SAGE1, CT45A1, CT45A4, CT45A6, GAGE1, NXF2B, SPANXN1, CT45A3, CT45A2, PAGE3, SPANXN2, SPANXA2, MAGEA9B, MAGEA8, MAGEA6, GAGE13, PAGE4, PAGE5, PAGE2, TAF7L, SPANXC, CTAG1B, FATE1, GAGE12J, TIGIT, MAGEA11, XAGE1D, PAGE2B, MAGEA9B, SPANXN5, SPANXN4, SPANXN3, TFDP3, MAGEA12, MAGEA10, CMKLR1, SSX7, SSX4, SSX5, SSX2, SSX3, NXF2, MAGEC1, MAGEC3, MAGEC2, PASD1,*

CTAG2, XAGE3, LUZP4, GAGE12D, GAGE12F, ZNF645, CT47A7, CT47A2, CT47A1, CT47B1, AKAP4, MAGEA3, MAGEA2, CT47A6, GAGE2A, MAGEB2, MAGEB3, MAGEB1, MAGEB4, PAGE1, XAGE5, FMR1NB, FAM133A, CSAG2, CSAG1, CPXCR1, FTHL17, VENTXP1, DDX53, CT47A11, CT47A10, ARX, OIP5, SPATA19, PBK, IGSF11, MPHOSPH10, CEP55, NR6A1, TPPP2, TSPY2, SPEF2, CALR3, TEX15, TEX14, TEKT5, CAGE1, ODF3, ODF2, ODF1, ODF4, EFEMP1, TMEFF2, ADAM2, SPO11, PRM1, PRM2, PTPN20A, CTAGE1, CTAGE5, CASC5, CTNNA2, DKKL1, BRDT, SEMG1, RGS22, FBXO39, MORC1, DCAF12L2, PRSS54, PRAME, MAEL, POTEH, POTEG, POTEE, POTED, POTEB, POTEC, TTK, TMPRSS12, DNAJB8, ADAM29, TSPY1, NLRP4, NAGLU, HSPA4L, SLCO6A1, CCDC83, ACRBP, ZNF165, ANKRD45, SPAG8, SPAG9, SPAG6, SPAG1, GPAT2, DMRT1, SPACA3, DSCR8, LEMD1, CCDC33, CCDC36, CTCFL, DPPA2, TDRD12, SYCE1L, NOL4, WT1, CCDC62, CRISP2, HORMAD2, HORMAD1, CEP290, KIAA0100, TSGA10, TSSK6, AKAP3, SPAG17, SYCP1, DDX43, LIPI, ACTL8, COX6B2, TEX101, GPATCH2, ATAD2B, HSPB9, PIWIL2, CABYR, RBM46, PRSS55, SPAG4, SPA17, TDRD6, LY6K, ARMC3, ELOVL4, OTOA, THEG, and *TULP2* [1]. The full ISG panel included the following genes: *IL2RG, CD27, UBA7, DUSP18, PDCD1LG2, RNASEH2A, HLA-DOA, JAK1, CCR5, CXCR6, RSAD2, SAMHD1, PRF1, TIGIT, CD276, IFIH1, PSMB10, IFI16, HLA-E, CD8A, CMKLR1, LRIG1, LHB, IFNGR1, LAG3, IFI27L1, CD3D, CD3E, IFNW1, HLA-DRB1, NKG7, CXCL9, LY6E, CCL5, TREX1, IFI44L, CIITA, IFNAR2, IFNAR1, FOXA1, DNASE1L1, DNASE1L3, CD274, IFITM1, IFIT3, OAS1, OASL, IFIT1, ISG15, IRF7, IRF5, IRF9, IDO1, CXCL11, CXCL10, TLR3, TLR7, TLR9, GZMA, SLAMF6, TRIP10, C1QA, SERPING1, HLA-DRA, HMX1, STAT1* [2-6]. From this comprehensive panel, we derived a focused 15-gene brief ISG signature based on recent clinical trial evidence [2, 3], comprising *IFI27L1, IFI44L, IFIT1, RSAD2, SIGLEC1, STAT1, CXCL9, CXCL10, HLA-DRA, GZMA, PRF1, IDO1, CXCL11, CCR5, IFNG*.

Statistics and Analysis

A fundamental challenge in cluster analysis involves determining the optimal number of clusters, a problem that remains unresolved in the field [7, 8]. For hierarchical agglomerative clustering methods, this challenge directly relates to establishing appropriate stopping criteria for the clustering process. Without predefined stopping rules, the algorithm continues merging cluster pairs until all elements consolidate into a single cluster containing all elements [8, 9]. Dendrograms provide visual representations of agglomerative clustering results, with each level corresponding to a specific step in the clustering process. The internal nodes of these dendrograms represent roots of subtrees containing sample elements grouped at each iteration, forming "current clusters" [9]. Each dendrogram level serves as the input set for subsequent clustering iterations.

The existence of multiple clustering algorithms introduces challenges regarding clustering stability. For our analysis, we implemented hierarchical gene expression clustering using Ward's method with established stopping rules [10, 11]. We hypothesized that optimal clustering should demonstrate biological relevance, therefore limiting our analysis to the two most informative intervals of agglomerative clustering.

We generated gene distribution histograms enabling visual assessment of expression patterns across melanoma patients. We additionally created and analyzed heat maps to characterize clusters. Statistical evaluation of relationships between clustered gene groups incorporated Pearson's chi-square test, lambda coefficient, contingency coefficient, phi coefficient, Goodman and Kruskal's tau, uncertainty coefficient, and column proportion analysis. Analyses were performed using IBM SPSS Statistics v.26 and Python 3 libraries (pandas, numpy, matplotlib, seaborn, and scikit-learn). We applied Bonferroni correction for multiple comparisons, considering corrected p-values < 0.05 statistically significant.

Results

CTA Cauterization

The histogram analysis of CTA gene expression distribution revealed several genes exhibiting bimodal expression patterns, including *MAGEA6, PAGE5, MAGEA11, XAGE1D, MAGEA10, MAGEA12, MAGEC1, MAGEC2, CTAG2, MAGEA3, MAGEA2, CSAG2, CSAG1, CTNNA2, DSPCR8, CCDC36, HORMAD1, SEP290, DDX43, LY6K*. These bimodal distributions suggested the existence of two distinct patient subgroups characterized by either high or low CTA gene activity. We excluded PRAME from subsequent cluster analyses to enable more meaningful patient stratification consistent with its established role as a melanoma-specific marker (fig. 1).

The analysis generated dendrograms and heat maps visualizing gene expression patterns (fig. 2).

Our analysis identified six primary CTA clusters at the first hierarchical level and ten subclusters at the third level (second level was omited as noninformative). Clusters 1 and 2 (AllRedPart#1 and AllRedPart#2) demonstrated minimal expression across most CTA genes, with Cluster 1 showing particularly low activity of *MAGEA6, MAGEA12, MAGEC1, MAGEC2, MAGEA3, CTNNA2*. Clusters 3–6 exhibited elevated CTA expression, with *MA-*

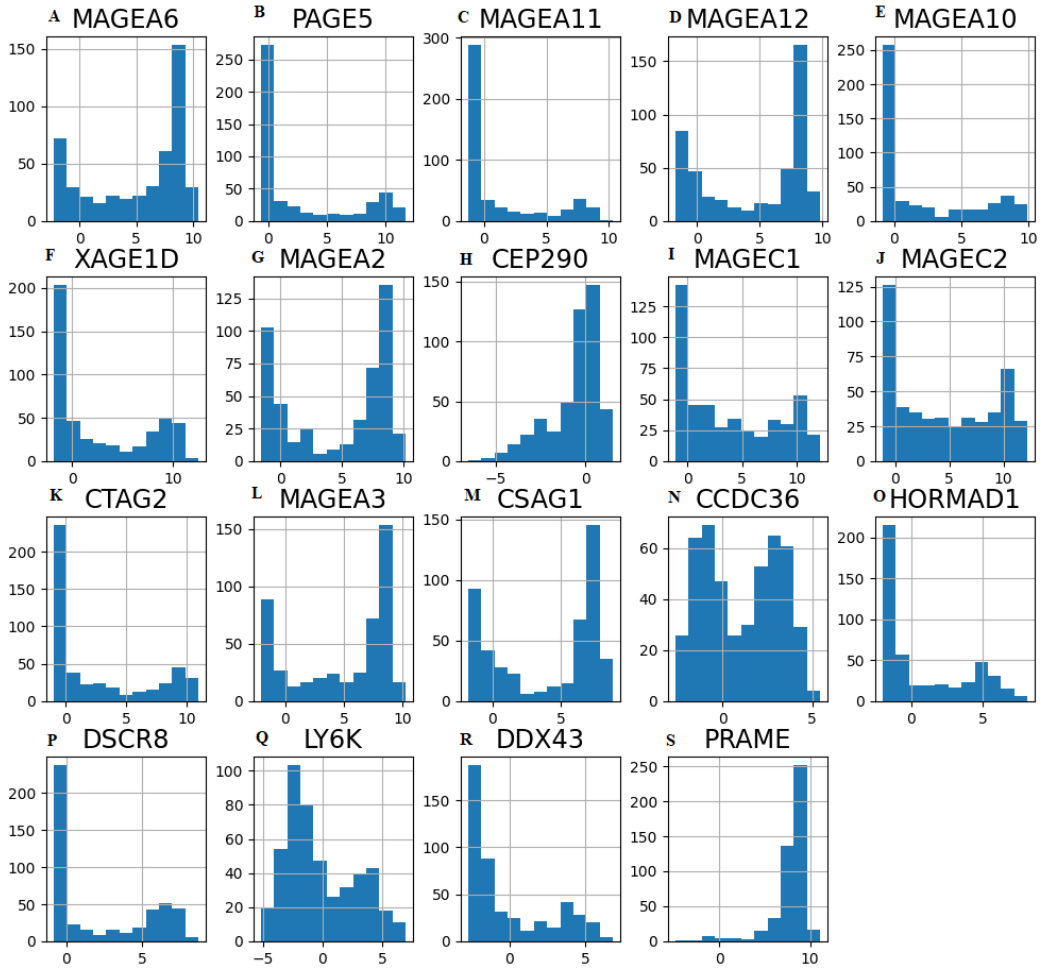

Fig. 1. Expression histograms of cancer-testis antigens (CTA) in melanoma specimens: 1, A) *MAGEA6*; 1, B) *PAGE5*; 1, C) *MAGEA11*; 1, D) *MAGEA12*; 1, E) *MAGEA10*; 1, F) *XAGE1D*; 1, G) *MAGEA2*; 1, H) *CEP20*; 1, I) *MAGEC1*; 1, J) *MAGEC2*; 1, K) *CTAG2*; 1, L) *MAGEA3*; 1, M) *CSAG1*; 1, N) *CCDC36*; 1, O) *HORMAD1*; 1, P) *DSCR8*; 1, Q) *LY6K*; 1, R) *DSCR8*; 1, S) *DDX43*; 1, T) *PRAME*

GEA6, MAGEA12, MAGEA3, MAGEA2, CSAG2, and *CSAG1* serving as key discriminators between high- and low-expression groups. Clusters 3 and 4 showed moderate *CTA* expression overall, with Cluster 4 displaying higher *CTAG2* expression but reduced *MAGEC1/MAGEC2* levels. Cluster 5 demonstrated the highest overall *CTA* activity, while Cluster 6 showed similar patterns but with reduced expression of *PAGE5, XADE10*, and *CTAG2* (see Supplementary table S1, online).

ISG clustering

The histogram analysis of ISG expression patterns revealed a unimodal distribution across all examined genes.

Cluster analysis identified four distinct ISG expression profiles (fig. 3). Notably, *LRIG1* and *FOXA1* showed no detectable expression in any cluster. The ISGHyper#2 cluster exhibited hyperexpression of most interferon-regulated genes, while ISGhigh#1 demonstrated similar characteristics with moderately reduced expression levels. ISGnon#3 displayed minimal gene expression, and ISGlow#4 showed slightly elevated expression relative to ISGnon#3 (Supplementary Table S2, online).

Parallel analysis of the brief ISG panel similarly identified four clusters (fig. 3). Clusters ISGb_non#1.1 and ISGb_low#1.3 shared comparable characteristics, though ISGb_non#1.1 showed complete absence of interferon-dependent gene expression. The ISGb_hyper#1.2 cluster demonstrated marked gene hyperexpression, while ISGb_high#1.4 exhibited similar but attenuated expression patterns. Comparative analysis revealed strong concordance between the full and brief ISG clustering results, with significant correlation coefficients ($\lambda = 0.666$, $p = 6\times10^{-61}$; symmetric uncertainty coefficient = 0.56, $p = 8\times10^{-151}$). We utilized the brief ISG panel for subsequent analyses (Supplementary Table S2, online).

Interaction Between ISG and CTA Clusters

Initial comparison of first-level clusters revealed no significant association between ISG and CTA expression patterns ($p > 0.1$). However, analysis of third-level CTA clusters against the brief ISG signature demonstrated a weak correlation (symmetric uncertainty coefficient = 0.031, $p = 0.003$; ISG-dependent uncertainty coefficient = 0.025, $p = 0.003$), as detailed in table 1.

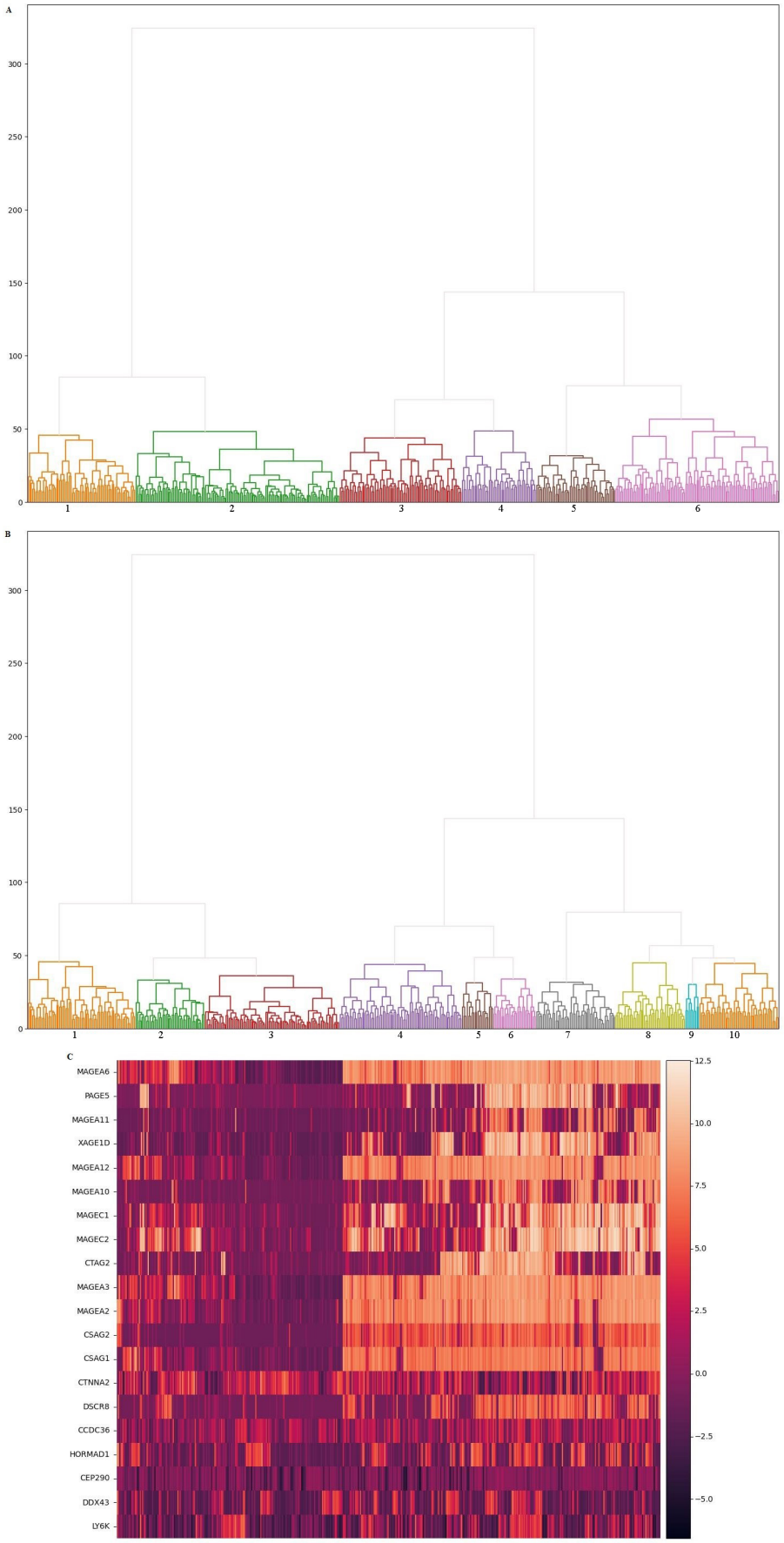

Fig. 2. The hierarchical clustering results of *CTA* gene expression in melanoma, with color-coded clusters. The x-axis represents individual patients, maintaining consistent patient alignment across all panels (A–C). 2, A — dendrograms of the cluster analysis (level 1); 2, B — dendrograms of the cluster analysis (level 3); 2, C — gene expression heatmap. Darker colors indicate lower expression levels

Only two third-level CTA clusters exhibited meaningful associations with ISG patterns: one characterized by minimal CTA expression and another showing high expression across all CTA genes. We hypothesize that in the first case, robust immune system activity may lead to complete elimination of immunogenic CTA-expressing tumor cells, potentially representing an immune escape mechanism. This phenomenon could indicate the presence of potent antitumor or neoantigen-specific lymphocyte clones. Conversely, in case of high CTA expression alternative immune evasion strategies might be employed.

These findings suggest that different immunotherapy approaches might prove beneficial to the patients — a hypothesis requiring validation in prospective clinical trials.

The comprehensive comparison revealed a weak but statistically significant association between the two cluster groups. The uncertainty coefficient for ISG dependent variable was 0.042 and 0.05 for the symmetric association.

Discussion

The dynamic interplay between tumor cells and immune cells during tumorigenesis is mediated by endogenous type I and II interferons (IFNs) [19]. During the elimination phase, IFN-mediated recognition triggers chemokine and cytokine production in the tumor bed, establishing a positive feedback loop that amplifies immune cell recruitment — particularly NK cells and cytotoxic T lymphocytes— and subsequent IFN production.

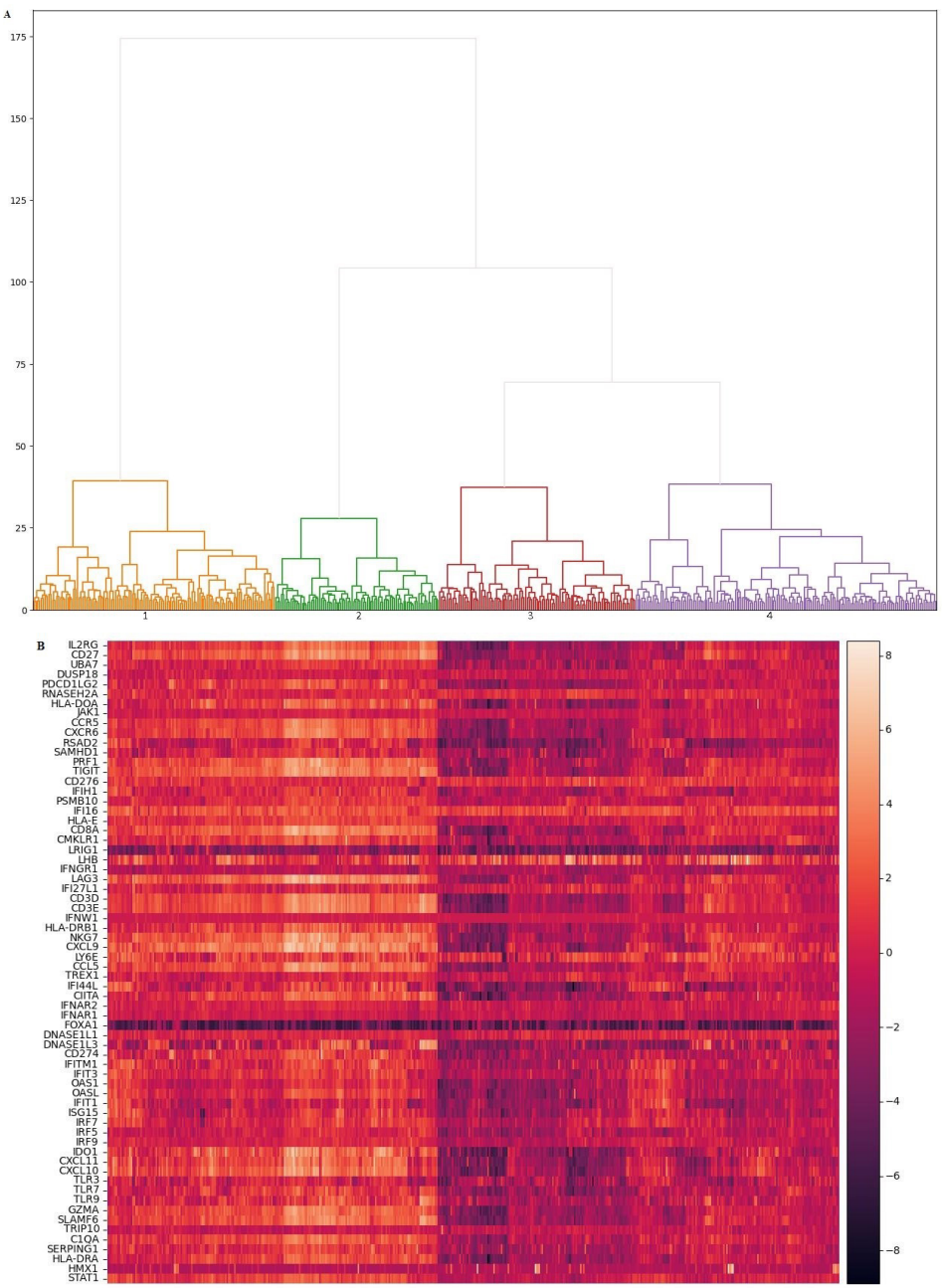

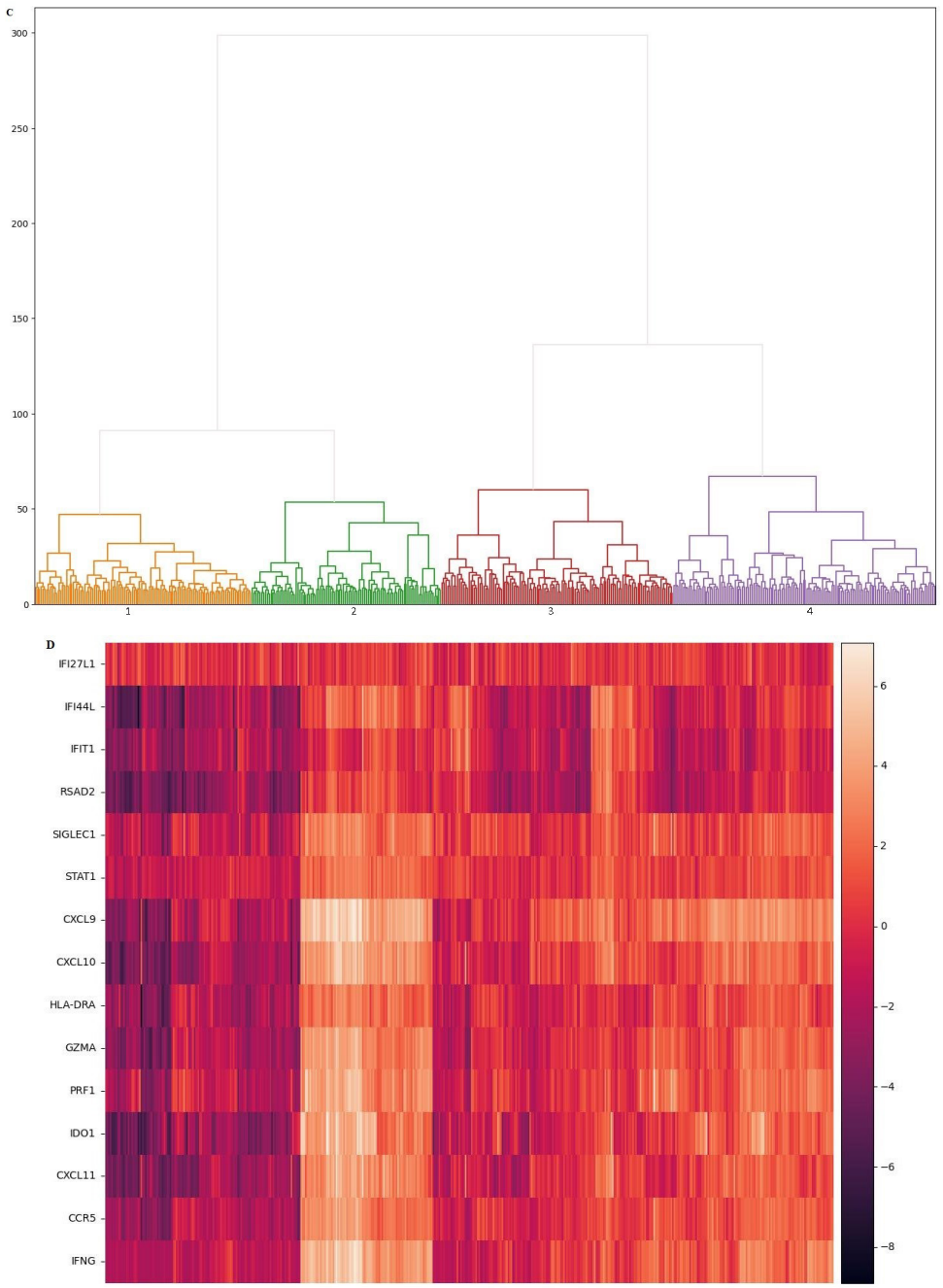

Fig. 3. Dendrograms and cluster analysis results of full and brief ISG signatures in melanoma specimens. 3, A) Clustering dendrogram of full ISG expression profiles; 3, B) Heatmap of full ISG expression patterns; 3, C) Dendrogram of the brief ISG cluster analysis; 3, D) Heatmap of the brief ISG. Darker color represent lower gene expression levels

Tumor cell sensitivity to IFN's possible direct cytotoxic effects further contributes to effective antitumor immunity.

Current classification systems recognize three distinct tumor microenvironment (TME) profiles based on $CD8^+$ T cell infiltration [12].

Patients with solid tumors with high checkpoint inhibitor responsiveness usually exhibit an active immune profile or so-called immune-inflamed ("hot") phenotype. On the other hand, non-responsive patients may exhibit "cold" phenotype with no immune infiltration. In addition, there is an immune phenotype located between the "cold" and "hot" categories, known as the immune-"excluded" type [13].

Our findings demonstrate four ISG clusters that stratify into high- and low-expression groups, corresponding to "hot" and "cold" tumor phenotypes respectively. The "hot" tumor phenotype is characterized by elevated ISG expression, while the "cold" type has low expression levels. Patients with elevated ISG expression may exhibit superior treatment responses, while those with "cold" tumors could benefit from dendritic cell vaccines (DCV) to enhance T cell infiltration and IFN saturation, as demonstrated by Bulgarelli J. et al. [14].

Table. Contingency table analysis of brief ISG clusters vs third-level CTA clusters

CTA clusters 100 %		Brief ISG Clusters							
		ISG_non#2.1		ISG_Hyper#2.2		ISG_low#2.3		ISG_high#2.4	
Level 1	Level 3	N	%[1]	N	%[1]	N	%[1]	N	%[1]
AllRed	AllRedPart #3.1	22[a]	32.4 %	1[a]	16.2 %	14[a]	20.6 %	2[a]	30.9 %
	AllRedPart #3.2	16[a]	36.4 %	8[a]	18.2 %	5[a]	11.4 %	15[a]	34.1 %
	AllRed #3.3	25[a,b]	29.4 %	8[b]	9.4 %	15[a.b]	17.6 %	37[a]	43.5 %
AllHigh Part 1	AllHighPart1 #3.4	22[a]	28.6 %	15[a]	19.5 %	16[a]	20.8 %	24[a]	31.2 %
AllHigh Part 2	AllHighPart2 #3.5	3[a]	15.0 %	2[a]	10.0 %	7[a]	35.0 %	8[a]	40.0 %
	AllHighPart2 #3.6	3[a]	11.1 %	4[a]	14.8 %	8[a]	29.6 %	12[a]	44.4 %
AllHyper	AllHyper #3.7	7[a]	14.0 %	18[b]	36.0 %	14[a.b]	28.0 %	11[a]	22.0 %
	AllHyperPart1 #3.8	7[a]	15.9 %	12[a]	27.3 %	11[a]	25.0 %	14[a]	31.8 %
	AllHyperPart2 #3.9	1[a]	11.1 %	0 [a]	0.0 %	4[a]	44.4 %	4[a]	44.4 %
	AllHyperPart3 #3.10	21[a]	42.0 %	8[a]	16.0 %	9[a]	18.0 %	12[a]	24.0 %

[1] The proportion within each CTA cluster; [a,b,c,d,e] each upper index signifies a subset of categories for brief ICG; where the proportions of rows do not differ significantly from each other at the $p < 0,05$; N — patient counts.

Melanoma is widely recognized as an immunogenic "hot" tumor type characterized by abundant $CD8^+$ T cell infiltration within the tumor microenvironment (TME) [15]. Thus, there is potential for immune-mediated tumor recognition and destruction. However, interpatient variability exists in both the quantity and functional activity of immune components in TME, contributing to the heterogeneous responses observed with immune checkpoint inhibitors. Furthermore, melanoma cells actively produce numerous immunosuppressive factors that depolarize the immune infiltrate, resulting in TMEs enriched with pro-tumor macrophages, neutrophils, and lymphocytes [24]. Our ISG clustering results confirm this biological spectrum, demonstrating that melanomas exist along a continuum from "cold" to "hot" phenotypes, with some tumors exhibiting mixed characteristics.

CTAs comprise a large family of tumor-associated proteins whose physiological expression is typically restricted to testicular germ cells (spermatogonia and spermatocytes) during proliferation. While CTA expression has been well-documented across various malignancies, significant variation exists within tumor types. Malignancies can be stratified by CTA expression frequency, with high-expressors (≥ 50 % frequency) including melanoma, lung cancer, hepatocellular carcinoma, germ cell tumors, gastric cancer, and chondrosarcoma. Conversely, leukemias, lymphomas, kidney cancer, glioblastoma, and colorectal carcinoma typically demonstrate low CTA expression (< 20 %) [16].

Traditionally, it is believed that CTA contribute to multiple oncogenic processes by promoting proliferative signaling, apoptosis resistance, metabolic reprogramming, invasion/metastasis, angiogenesis, genomic instability and mutations accumulation [17]. Although associated with poorer clinical outcomes, CTAs possess high immunogenicity due to their absence from immune surveillance during adulthood, making them attractive targets for immunotherapy. CTAs are also involved in disrupting critical cellular aging pathways, enabling tumor cells bypass several key tumor-suppressive checkpoints. These antigens also induce epithelial-mesenchymal transition, thereby enhancing cancer cell migratory and invasive capacity. Additionally, CTA expression contributes to increased genomic instability [18].

We identified three main types of CTA expression, totaling six clusters at level 1, comprising two high-expression, two medium-expression, and two low-expression patterns. This expands upon our previous 2020 study that reported only four clusters [7]. With the expanded dataset enabled both validation of prior findings and discovery of two additional distinct CTA clusters. Given CTAs' established role as immunotherapeutic targets, we anticipate that future clinical applications will incorporate CTA cluster profiling to guide personalized treatment selection between immunotherapy and vaccine-based approaches, though this requires prospective clinical validation.

The tumor-specific expression patterns and oncogenic properties of CTAs make them particularly attractive therapeutic targets with minimal side effects.

Ayabe R.I. et al. (2024) conducted a study of CTA in samples of small intestinal neuroendocrine tumors. Uncontrolled clustering of gene expression demonstrated a dichotomy between high and low CTA expression. High-expressors demonstrated concurrent type I IFN upregulation (including PRAME, GAGE1, and MAGEA3) and superior overall survival compared to patients with low CTA, regardless of the stage [19]. The observed stromal NK cell activation in these tumors suggests an immune-mediated survival benefit associated with combined CTA/IFN type I expression.

In our cohort, analysis found no significant association between first-level ISG and CTA clusters ($p > 0.1$). However, third-level CTA cluster analysis demonstrated two weakly correlated patterns with brief ISG signatures: symmetric uncertainty coefficient 0.031, $p = 0.003$; ISG as dependent variable uncertainty coefficient 0.025, $p = 0.003$. Only two third-level CTA clusters clinically relevant associations with the ISG: AllRed#3.3 and AllHyper#3.7.

AllRed#3.3 cluster is marked by absent CTA expression alongside ISG high- and hyperexpression. This cohort of patients show high immune cell activity against a backdrop of a lack of targets for therapy. We propose that high activity of immune system led to the loss of all immunogen CTA in the first case. Perhaps CTA loss is the mechanism of immune escape here. So, there can be enough potent antitumor or neoantigen-specific lymphocyte clones. We hypothesize these patients represent optimal candidates for anti-PD-1 therapy.

AllHyper#3.7 cluster is characterized by CTA hyperexpression with low levels or absence of ISG expression. We observe a category of patients with low immune system activity against a backdrop of a large number of therapy targets (CTA). In case of high CTA expression probably other mechanisms of immune escape work. We propose that this ratio of CTA and ISG may be a predictive indicator of high efficacy in the use of vaccine therapies or antigen-presentation enhancement strategies. This method is an active specific immunotherapy based on stimulating tumor-specific responses.

These findings underscore the need for independent clinical evaluation of CTA and ISG expression patterns, since they represent independent units.

Conflict of interest
The authors declare no conflict of interest.

Funding
This study was conducted as part of the planned research program (RK 124020300020-0) of the N.N. Petrov National Medical Research Center of Oncology, a Federal State Budgetary Institution under the Ministry of Health of the Russian Federation, for the period 2024–2026.

Compliance with patient rights and principles of bioethics
Not applicable (online registry data was used).

Authors' contributions
All authors made a substantial contribution to the conception of the work, acquisition, analysis, interpretation of data for the work, drafting and revising the work, final approval of the version to be published and agree to be accountable for all aspects of the work.

ЛИТЕРАТУРА / REFERENCES

1. CTdatabase. Online database. Ludwig Institute for Cancer Research, Laboratorio National de Compulacao Cientifica. 2024.-URL: http://www.cta.lncc.br/ (01.06.2024).
2. Rozeman E.A., Hoefsmit E.P., Reijers I.L.M., et al. Survival and biomarker analyses from the OpACIN-neo and OpACIN neoadjuvant immunotherapy trials in stage III melanoma. Nat Med. 2021; 27(2): 256-263.-DOI: 10.1038/s41591-020-01211-7.-URL: https://www.ncbi.nlm.nih.gov/pubmed/33558721, https://www.nature.com/articles/s41591-020-01211-7.
3. Reijers I.L.M., Rao D., Versluis J.M., et al. IFN-γ signature enables selection of neoadjuvant treatment in patients with stage III melanoma. *The Journal of experimental medicine.* 2023; 220(5).-DOI: 10.1084/jem.20221952.-URL: https://rupress.org/jem/article-pdf/220/5/e20221952/1449193/jem_20221952.pdf.
4. Barrat F.J., Crow M.K., Ivashkiv L.B. Interferon target-gene expression and epigenomic signatures in health and disease. *Nature immunology.* 2019; 20(12): 1574-1583.-DOI: 10.1038/s41590-019-0466-2.-URL: https://pmc.ncbi.nlm.nih.gov/articles/PMC7024546/pdf/nihms-1556675.pdf.
5. Elnaggar M., Chaisuparat R., Ghita I., et al. Immuno-oncologic signature of malignant transformation in oral squamous cell carcinoma. *Oral Surg Oral Med Oral Pathol Oral Radiol.* 2023; 136(5): 612-622.-DOI: 10.1016/j.oooo.2023.07.009.
6. Bergamaschi C., Terpos E., Rosati M., et al. Systemic IL-15, IFN-γ, and IP-10/CXCL10 signature associated with effective immune response to SARS-CoV-2 in BNT162b2 mRNA vaccine recipients. *Cell Rep.* 2021; 36(6): 109504.-DOI: 10.1016/j.celrep.2021.109504.-URL: https://pmc.ncbi.nlm.nih.gov/articles/PMC8299183/pdf/main.pdf.
7. Орехов А.В. Марковский момент остановки агломеративного процесса кластеризации в евклидовом пространстве. *Вестник Санкт-Петербургского университета. Прикладная математика. Информатика. Процессы управления.* 2019; 15(1): 76-92.-DOI: 10.21638/11702/ spbu10.2019.106.-URL: http://hdl.handle.net/11701/15652. [Orekhov A.V. Markov moment for the agglomerative method of clustering in Euclidean space. *Petersburg University Applied Mathematics Computer Science Control Processes.* 2019; 15(1):76-92.-DOI: 10.21638/11702/ spbu10.2019.106.-URL: http://hdl.handle.net/11701/15652 (in Rus)].
8. Hartigan J.A. Clustering Algorithms. New York, London, Sydney, Toronto: John Wiley & Sons Inc. Press. 1975; 351.-URL: https://books.google.ru/books?id = cDnvAAAAMAAJ.-ISBN: 9780471356455.
9. Everitt B.S., Landau S., Leese M., Stahl D. Cluster Analysis. Chichester, West Sussex, UK: John Wiley & Sons Ltd. Press. 2011; 330.-URL: https://books.google.ru/books?id = w3bE1kqd-48C.-ISBN: 9780470978443.
10. Murtagh F., Legendre P. Ward's Hierarchical Agglomerative Clustering Method: Which Algorithms Implement Ward's Criterion? *Journal of Classification.* 2014; 31(3): 274–295.-DOI: 10.1007/s00357-014-9161-z.-URL: http://dx.doi.org/10.1007/s00357-014-9161-z.
11. Orekhov A.V. Quasi-Deterministic Processes with Monotonic Trajectories and Unsupervised Machine Learning. *Mathemat-*

ics. 2021; 9(18): 2301.-URL: https://www.mdpi.com/2227-7390/9/18/2301.

12. Binnewies M., Roberts E.W., Kersten K., et al. Understanding the tumor immune microenvironment (TIME) for effective therapy. Nature medicine. 2018; 24(5): 541-550.-DOI: 10.1038/s41591-018-0014-x.-URL: https://www.ncbi.nlm.nih.gov/pubmed/29686425.
13. Wu B., Zhang B., Li B., et al. Cold and hot tumors: from molecular mechanisms to targeted therapy. *Signal transduction and targeted therapy.* 2024; 9(1): 274.-DOI: 10.1038/s41392-024-01979-x.-URL: https://www.ncbi.nlm.nih.gov/pubmed/39420203.
14. Bulgarelli J., Tazzari M., Granato A.M., et al. Dendritic Cell Vaccination in Metastatic Melanoma Turns "Non-T Cell Inflamed" Into "T-Cell Inflamed" Tumors. *Frontiers in immunology.* 2019; 10: 2353.-DOI: 10.3389/fimmu.2019.02353.
15. Maleki Vareki S. High and low mutational burden tumors versus immunologically hot and cold tumors and response to immune checkpoint inhibitors. *Journal for immunotherapy of cancer.* 2018; 6(1): 157.-DOI: 10.1186/s40425-018-0479-7.-URL: https://www.ncbi.nlm.nih.gov/pubmed/30587233.
16. Naik A., Lattab B., Qasem H., Decock J. Cancer testis antigens: Emerging therapeutic targets leveraging genomic instability in cancer. *Mol Ther Oncol.* 2024; 32(1): 200768.-DOI: 10.1016/j.omton.2024.200768.-URL: https://www.ncbi.nlm.nih.gov/pubmed/38596293.
17. Gibbs Z.A., Whitehurst A.W. Emerging Contributions of Cancer / Testis Antigens to Neoplastic Behaviors. *Trends in cancer.* 2018; 4(10): 701-712.-DOI: 10.1016/j.trecan.2018.08.005.-URL: https://www.ncbi.nlm.nih.gov/pubmed/30292353.
18. Kurtenbach S., Sanchez M.I., Kuznetsoff J., et al. PRAME induces genomic instability in uveal melanoma. *Oncogene.* 2024; 43(8): 555-565.-DOI: 10.1038/s41388-023-02887-0.-URL: https://www.ncbi.nlm.nih.gov/pubmed/38030788.
19. Ayabe R.I., Seo Y.D., Melendez B., et al. Correlation of cancer testis antigen expression with high type-I interferon signal and prognosis in small bowel neuroendocrine tumors. *Journal of Clinical Oncology.* 2024; 42(3_suppl): 596-596.-DOI: 10.1200/JCO.2024.42.3_suppl.596.-URL: https://ascopubs.org/doi/abs/10.1200/JCO.2024.42.3_suppl.596.

Received / 24.07.2025
Reviewed / 31.07.2025
Accepted for publication / 04.09.2025

Author Information / ORCID

Aleksei V. Novik / ORCID ID: https://orcid.org/0000-0002-2430-4709.
Kristina Yu. Kapusta / ORCID ID: https://orcid.org/0009-0000-9037-3617.
Tatiana L. Nekhaeva / ORCID ID: https://orcid.org/0000-0002-7826-4861.
Anna B. Danilova / ORCID ID: https://orcid.org/0000-0003-4796-0386.
Andrey V. Orekhov / ORCID ID: https://orcid.org/0000-0001-7641-956X.
Egor V. Vasiliev / ORCID ID: https://orcid.org/0009-0000-3679.
Dilorom Kh. Latipova / ORCID ID: https://orcid.org/0000-0002-8906-0370.
Anna I. Semenova / ORCID ID: https://orcid.org/0000-0003-4538-8646.
Lilia S. Baboshkina / ORCID ID: https://orcid.org/0000-0002-5079-3382.
Gulfiya M. Teletaeva / ORCID ID: https://orcid.org/0000-0001-9365-8554.
Tatiana Yu. Semiglazova / ORCID ID: https://orcid.org/0000-0002-4305-6691.
Irina A. Baldueva / ORCID ID: https://orcid.org/0000-0002-7472-4613.